



# Pseudo-ductility in intermingled carbon/glass hybrid composites with highly aligned discontinuous fibres



HaNa Yu<sup>\*</sup>, Marco L. Longana, Meisam Jalalvand, Michael R. Wisnom, Kevin D. Potter

Advanced Composites Centre for Innovation and Science, University of Bristol, Queen's Building, University Walk, Bristol BS8 1TR, UK

## ARTICLE INFO

### Article history:

Received 29 October 2014

Received in revised form 4 February 2015

Accepted 14 February 2015

Available online 5 March 2015

### Keywords:

A. Hybrid

A. Discontinuous reinforcement

B. Fragmentation

E. Preform

## ABSTRACT

The aim of this research is to manufacture intermingled hybrid composites using aligned discontinuous fibres to achieve pseudo-ductility. Hybrid composites, made with different types of fibres that provide a balanced suite of modulus, strength and ductility, allow avoiding catastrophic failure that is a key limitation of composites. Two different material combinations of high strength carbon/E-glass and high modulus carbon/E-glass were selected. Several highly aligned and well dispersed short fibre hybrid composites with different carbon/glass ratios were manufactured and tested in tension in order to investigate the carbon ratio effect on the stress–strain curve. Good pseudo-ductile responses were obtained from the high modulus carbon/E-glass composites due to the fragmentation of the carbon fibres. The experimental results were also compared with an analytical solution. The intermingled hybrid composite with 0.25 relative carbon ratio gave the maximum pseudo-ductile strain, 1.1%, with a 110 GPa tensile modulus. Moreover, the initial modulus of the intermingled hybrids with 0.4 relative carbon ratio is 134 GPa, 3.5 times higher than that of E-glass/epoxy composites. The stress–strain curve shows a clear “yield point” at 441 MPa and a well dispersed and gradual damage process.

© 2015 The Authors. Published by Elsevier Ltd. This is an open access article under the CC BY license (<http://creativecommons.org/licenses/by/4.0/>).

## 1. Introduction

Hybrid composites consist of two or more types of fibres in a common matrix and it is possible to control modulus and strength of the material by modulating the relative ratio of the fibres. Based on the distribution of each constituent, continuous and discontinuous fibre hybrid composites can be categorised into three major types [1–4], as shown in Fig. 1:

- Interlaminated hybrids, where the hybridisation is achieved at laminate level by stacking plies of different constituents.
- Intraply or intrayarn hybrids, where different bundles are mixed within the layers in parallel or different yarns or bundles are co-woven.
- Intermingled hybrids, where different types of constituents are intimately mixed and the hybridisation is achieved within the ply.

Continuous fibre reinforced hybrid composites are commonly used where high structural performance and economic efficiency are required. The mechanical properties and damage modes of

continuous fibre reinforced hybrid composites as a function of the ratio between different fibres and dispersion state were investigated and reported by several researchers. Two interesting phenomena are typically observed. One is that the first failure occurs in the lower elongation constituent at a certain strain [5–11], which results in knee points in the stress–strain curve. The other one is known as the “synergistic strengthening” or “hybrid effect”. This is defined in different ways by different researchers [2,4,7,12–14], but the crucial observation is that the failure strain, and hence the strength, of the low elongation constituent appears to be greater in hybrid than in pure-low elongation fibre composite materials. Aveston et al. [5,6] suggested the theory of multiple matrix cracking and constrained failure for composites where the matrix fails before the fibres when loaded in tension. They provided a theoretical basis for the computation of the mechanical properties of hybrid composites and applied it to several case studies such as carbon fibre reinforced cement composites, interlaminated carbon/glass specimens, and glass/epoxy crossply laminate [6]. Bader and Manders [7,13] evaluated the tensile properties of interlaminated hybrid composites fabricated from glass and carbon fibres in an epoxy matrix to establish the role of glass–carbon ratio and the level of dispersion in determining the extent of the hybrid effect. They found that the apparent failure strain of the carbon phase increased as the relative carbon ratio was decreased, and

<sup>\*</sup> Corresponding author.

E-mail address: [Hana.Yu@bristol.ac.uk](mailto:Hana.Yu@bristol.ac.uk) (H. Yu).

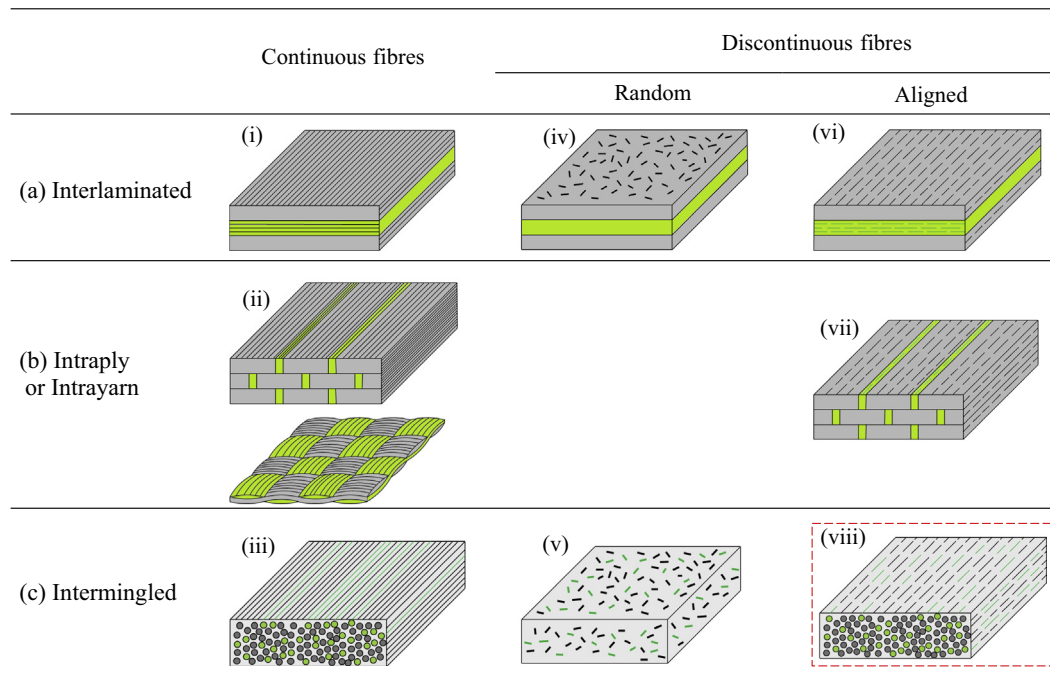


**Fig. 1.** Hybrid configurations for continuous and discontinuous fibre reinforced composites. (This research studies on (vii) in the red box.). (For interpretation of the references to colour in this figure legend, the reader is referred to the web version of this article.)

as the carbon fibre was more finely dispersed. However, despite the benefits of hybridisation, the transition between the elastic deformation and the damage evolution regions has normally been abrupt. Recently, a smooth transition between those two regions was achieved using very thin carbon plies at the University of Bristol [15–18]. The aim was to understand and control the damage process of continuous unidirectional hybrid materials and hence to achieve pseudo-ductile tensile response. Interlaminated hybrids with continuous glass and carbon fibres in epoxy matrix have been designed to avoid catastrophic failure due to delamination between the carbon and glass layers [15–18]. Multiple carbon fibre fractures (fragmentation) and stable propagation of delamination were achieved by selecting the right thickness and ratio for the carbon and glass layers. Damage mode maps were generated to study the effects of absolute and relative thickness of the carbon layers; these proved to be a very efficient design tool for hybrid composites [16,17].

Randomly distributed discontinuous fibre reinforced hybrid composites, Fig. 1(iv) and (v), are usually used for additional functions such as improvement of wear characteristics or electromagnetic shielding rather than structural applications [19,20]. However, high structural performance and good fibre dispersion can be achieved in discontinuous fibre composites with good fibre alignment processes. In particular, fluid based discontinuous fibre alignment processes can deal with short fibres individually: a more uniform hybridisation can be achieved compared to intermingled hybrid composites with continuous fibres [10,21,22]. As regards continuous intermingled hybrid composites, shown in Fig. 1(iii), a really good dispersion has never been achieved previously [23–25]. Richter [8] produced and tested hybrid composites with aligned discontinuous carbon and glass fibres by the VAF (vacuum-drum-filter) alignment-process. He compared interlaminated and intermingled hybrid composites with the same carbon/glass ratio: the two configurations showed approximately the same values for elastic modulus and impact strength but the intermingled hybrid composite was largely superior in flexural and tensile strength. Therefore, the intermingled hybrid composite with

aligned discontinuous fibres, shown in Fig. 1(viii), is probably the most interesting configuration that can give the finest dispersion whilst sustaining reasonable structural performance.

The aim of this research is to manufacture intermingled hybrid composites using aligned discontinuous fibres to investigate the stress–strain curves under tension and particularly in order to achieve pseudo-ductility through fragmentation of the lower elongation constituent. The HiPerDiF (High Performance Discontinuous Fibres) method, recently developed at the University of Bristol [26], is a unique fibre orientation method that uses the momentum change of fibres suspended in a low-viscosity fluid to achieve high level fibre alignment [27,28]. It was previously noted that tensile modulus, strength and failure strain of aligned discontinuous fibre composites were close to those of continuous fibre composites provided that the fibres are accurately aligned and their length is sufficiently long compared to the critical fibre length [26,29,30]. This novel process can also produce a wide range of hybrid preforms or prepregs with different fibre mixing ratios. In this paper, the overall stress–strain response of intermingled hybrid composites is investigated, demonstrating the feasibility of manufacturing fully intermingled hybrid composites with variations of fibre type and fibre ratios by the HiPerDiF method. To analyse the experimental results, the modelling approach developed by Jalalvand et al. [16] for continuous fibre hybrids is applied to intermingled aligned short fibre hybrid composites. The experimental results show that combining high modulus carbon and E-glass can result in a very good pseudo-ductile tensile response.

## 2. Intermingled hybrid composites

### 2.1. Discontinuous fibre alignment method

The HiPerDiF process for producing highly aligned discontinuous fibre preforms can be summarised in the following steps. Firstly, short fibres are dispersed in a liquid medium (water) that is accelerated through a nozzle; this partially aligns the fibres. As shown in Fig. 2(a), the fibre suspension jet is directed to the

orientation head which is comprised of two parallel plates with a controllable gap,  $d$ . The fibres are therefore aligned transversely to the suspension jet by a sudden momentum change of the liquid, provided that  $d$  is less than the fibre length. Subsequently, the water is removed through the perforated conveyor belt by a suction plate whilst maintaining the fibre orientation. The aligned fibre preform is dried to allow the resin impregnation process.

This modular structure, shown in Fig. 2(a), allows the orientation head size to be extended by placing several alignment units side by side in an array. It is therefore possible to create a short fibre tow or tape of a desired width and increase the production rate. This method enables manufacturing of different types of discontinuous fibre hybrid, as shown in Fig. 1(vi) to (viii), with various combinations of type, length and mixing pattern of fibres. The HiPerDiF method can achieve aligned short fibre preforms with a high level of hybridisation provided that the dispersion of the fibre mixture in the water is high enough; Fig. 2(b) shows a pictorial view of an intermingled hybrid based on two fibre types of the same length. In the prototype rig, the orientation head comprises two single units with two fibre suspension jets and enables manufacture of a 1 mm wide aligned discontinuous fibre preform.

## 2.2. Analytical model for intermingled hybrid composites

In this paper, hybrid composites are defined as a single matrix reinforced by two types of short fibres with different properties, i.e. glass and carbon. If the fibres are long compared to the critical length, then the same analytical assumption can be applied as for continuous fibre hybrids. In predicting the stress–strain response

of any hybrid composites with pseudo-ductile behaviour, a simple criterion has to be considered: the high elongation constituent should withstand the total load when the low elongation constituent breaks at the first cracking strain, as in Eq. (1) below [5,17],

$$\sigma_{@L\text{Frag}} = S_L \frac{\alpha\beta + 1}{\alpha(\beta + 1)} < \sigma_{@HF} = \frac{S_H}{1 + \beta} \quad \left( \alpha = \frac{E_L}{E_H}, \beta = \frac{V_L}{V_H} \right) \quad (1)$$

where  $\sigma_{@L\text{Frag}}$  is the overall stress in the specimen at the failure or fragmentation of the low elongation constituent (subscript  $L$ ) and  $\sigma_{@HF}$  is the stress in the specimen at failure of the high elongation constituent (subscript  $H$ ).  $S$ ,  $E$  and  $V$  are respectively the tensile strength, the tensile modulus and the volume fraction of each of the constituents. It is assumed that there is no concentration of stress on the high elongation constituent when the low elongation constituent breaks. If Eq. (1) is satisfied and the composite is strained above the failure strain of the low elongation constituent, a series of parallel cracks appears in the low elongation constituent. The spacing of cracks depends on the low and high elongation constituent properties, the shear yield stress of the matrix as well as the size of the low elongation constituent unit (fibre diameter, bundle diameter or lamina thickness). The formation of a single crack results in relaxation of the broken low elongation constituent and additional loads in the surrounding high elongation constituent. This leads to a stiffness reduction of the hybrid composite and extension of the specimen at a constant stress level.

For predicting the stress–strain response, the stress criterion for the fragmentation mode in hybrids with a simple sandwich structure (UD hybrids) developed in [17] was applied. Since the fibre length (3 mm) is long compared with the typical critical fibre

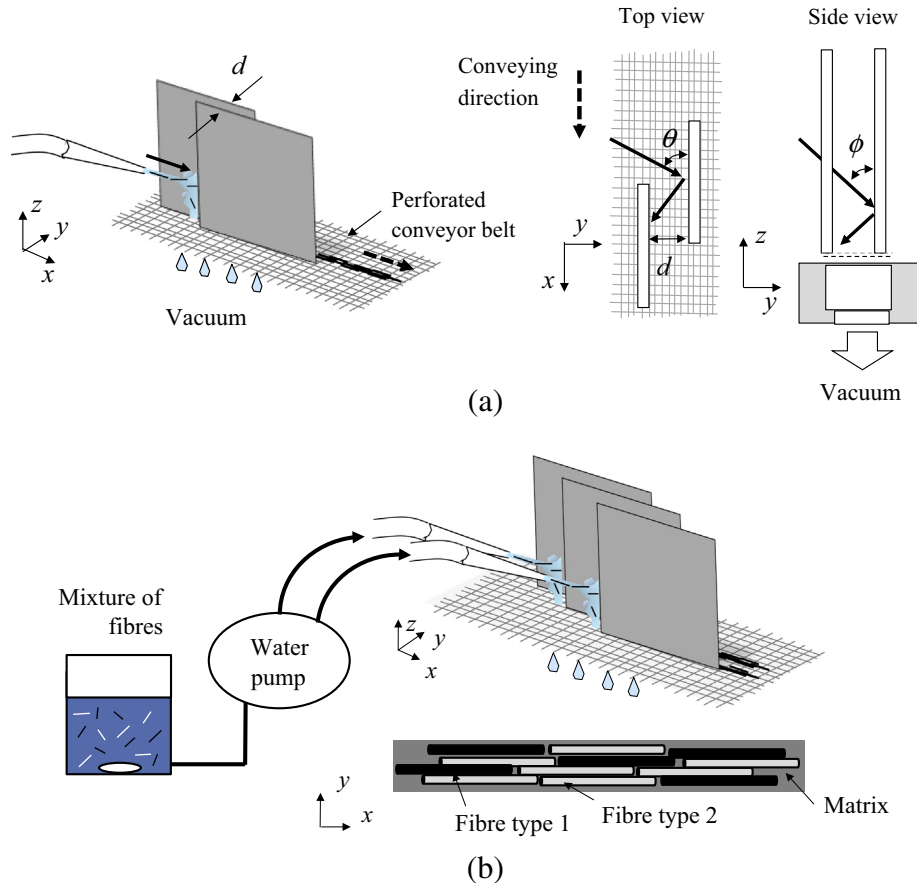


**Fig. 2.** (a) Single unit of orientation head of the HiPerDiF method, (b) idealisation of intermingled hybrid composite samples [26]. (For interpretation of the references to colour in this figure legend, the reader is referred to the web version of this article.)

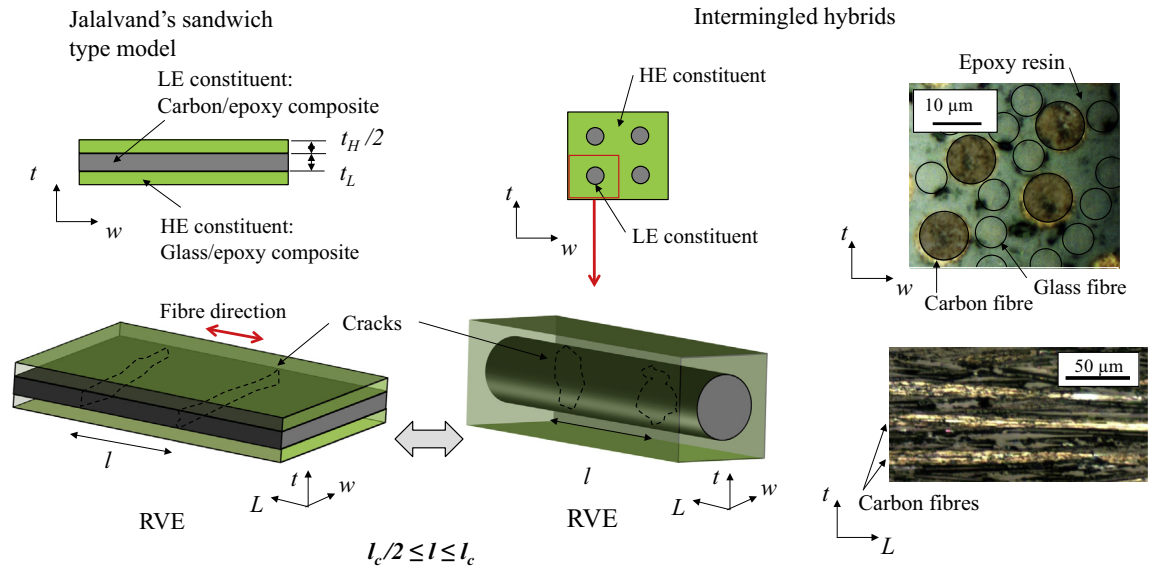


**Fig. 3.** Simplified modelling concept of intermingled hybrids comparing with the Jalalvand sandwich type model. (RVE: Representative volume element with length  $2l$ ). (For interpretation of the references to colour in this figure legend, the reader is referred to the web version of this article.)

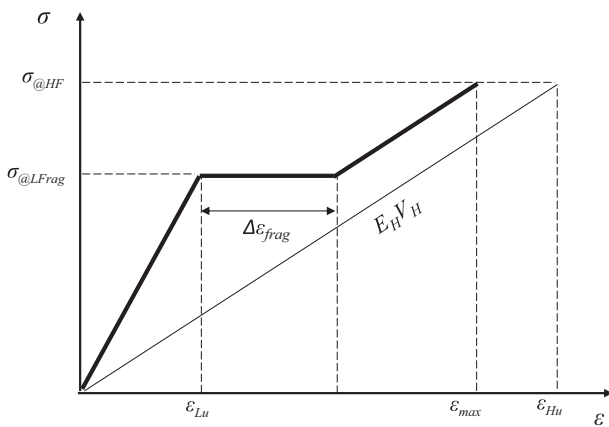


**Fig. 4.** Schematic stress–strain curves of hybrids with fragmentation in the low elongation constituent.

length (less than 0.5 mm) of carbon/epoxy composites, it can be assumed that the aligned discontinuous fibre composites behave like continuous UD composites. Extending Jalalvand's sandwich type model, a cylinder type-carbon constituent in a cube-type glass constituent arrangement was assumed as the representative volume element, as shown in Fig. 3. Since the dimensions of both the high and low elongation constituents are low in this representative volume element, no delamination is expected and the ratio of the low to high elongation constituent is the main effective parameter. Therefore these intermingled hybrid composites are expected to show a stable fragmentation rather than a catastrophic failure in their stress–strain response when the high elongation constituent can withstand the whole load after the failure of the low elongation constituent. The strain at which fragmentation initiates was also predicted with the Jalalvand model. The model assumes that there is a random variation of crack spacing,  $l_c/2 \leq l \leq l_c$ , where  $l_c$  is the critical length of the low elongation constituent.

**Table 1**  
Fibre and single-aligned discontinuous fibre composite specifications.

Manufacturer (brand name)		TohoTENAX (HTS)	NGF (Granoc, XN90)	Vetrotex (C100)
Fibres <sup>a</sup>	Fibre materials	PAN based high strength carbon	Pitch based high modulus carbon	E-glass
	Fibre length (mm)	3	3	3
	Density (g/cm <sup>3</sup> )	1.82	2.21	2.60
	Diameter (μm)	7	10	7
	Tensile strength (MPa)	4344	3430	2400
	Tensile modulus (GPa)	225	860	73
	Strain to fail (%)	1.93	0.398	3.29
	Sizing materials	Water soluble polymer	Unsize <sup>b</sup>	Starch/oil
Composites <sup>c</sup>	Fibre volume fraction (%)	55	–	55
	Tensile modulus (GPa)	115 ± 9.1	–	37.7 ± 2.2
	(±1 SD, CV%)	(7.9)	–	(5.9)
	Tensile strength (MPa)	1510 ± 112	–	740 ± 11.8
	(±1 SD, CV%)	(7.4)	–	(1.6)
	Strain to failure (%)	1.41 ± 0.14	–	1.97 ± 0.13
	(±1 SD, CV%)	(9.9)		(6.6)

<sup>a</sup> Tensile strength, modulus and failure strain are from the continuous fibre properties provided by the manufacturers.

<sup>b</sup> Fibres are originally sized with epoxy based materials. The sizing material is then removed by burning off method.

<sup>c</sup> Aligned discontinuous fibre composite properties were measured at University of Bristol, Yu [26].

**Table 2**

Process variables of the HiPerDiF method to manufacture hybrid-aligned short fibre preforms.

Relative high strength carbon ratio		0.1		0.2	
<i>Using two peristaltic pumps</i>					
Total fibre suspension flow rate ( $q$ )				4.46 ml/s	
Preform width ( $w$ )				$1 \times 10^{-3}$ m	
Perforated weave moving velocity ( $V_m$ )		$2.5 \times 10^{-3}$ m/s		$2.7 \times 10^{-3}$ m/s	
Fibre volume fraction in the suspension ( $v_{fs}$ )		Carbon	0.0007%	0.002%	
		Glass	0.008%	0.008%	
Fibre preform areal density (narrow tape type)		197 g/m <sup>2</sup>		202 g/m <sup>2</sup>	
<i>Using fibre preforms(tape type) for one composite sample</i>					
Number of fibre preforms in thickness direction				2	
Total preform areal density		394 g/m <sup>2</sup>		404 g/m <sup>2</sup>	
Avg. thickness of composites after curing		250 $\mu$ m		250 $\mu$ m	

Relative high modulus carbon ratio		0.1	0.2	0.25	0.33	0.4	0.5
<i>Using two peristaltic pumps</i>							
Total fibre suspension flow rate ( $q$ )				4.46 ml/s			
Preform width ( $w$ )				$1 \times 10^{-3}$ m			
Perforated weave moving velocity ( $V_m$ )				$2.5 \times 10^{-3}$ m/s			
Fibre volume fraction in the suspension ( $v_{fs}$ )		Carbon	0.0007%	0.0015%	0.002%	0.0025%	0.003%
		Glass	0.008%	0.006%	0.006%	0.005%	0.0045%
Fibre preform areal density (narrow tape type)			199 g/m <sup>2</sup>	169 g/m <sup>2</sup>	178 g/m <sup>2</sup>	165 g/m <sup>2</sup>	163 g/m <sup>2</sup>
							172 g/m <sup>2</sup>
<i>Using fibre preforms (tape type) for one composite sample</i>							
Number of fibre preforms in thickness direction				2			
Total preform areal density			398 g/m <sup>2</sup>	337 g/m <sup>2</sup>	357 g/m <sup>2</sup>	330 g/m <sup>2</sup>	327 g/m <sup>2</sup>
Avg. thickness of composites after curing			290 $\mu$ m	230 $\mu$ m	260 $\mu$ m	230 $\mu$ m	210 $\mu$ m
							220 $\mu$ m

An example of the expected stress–strain curve of hybrid composites with fragmentation in the low elongation constituent is shown in Fig. 4. The estimated additional strain during fragmentation ( $\Delta\epsilon_{frag}$ ) in the low elongation constituent and the maximum strain of the hybrid composites ( $\epsilon_{max}$ ) can be summarised from [17] and rewritten as in Eq. (2),

$$\Delta\epsilon_{frag} = \frac{11}{18} \epsilon_{Lu} \frac{E_L V_L}{E_H V_H} = \frac{11}{18} \epsilon_{Lu} \alpha \beta \quad (2a)$$

$$\epsilon_{max} = \epsilon_{Hu} - \frac{7}{18} \epsilon_{Lu} \alpha \beta \quad (2b)$$

where  $\epsilon_{Lu}$  and  $\epsilon_{Hu}$  are the failure strains of the low elongation constituent and the high elongation constituent respectively. When multiple fracturing of the low elongation constituent is complete,

i.e. after the plateau in the stress–strain curve shown in Fig. 4, the tensile modulus becomes  $E_H V_H$ .

### 3. Experiments

#### 3.1. Materials and specimen manufacturing

Data on fibres and composites with aligned discontinuous fibres are listed in Table 1 [26]. Before manufacturing and testing aligned discontinuous fibre hybrid composites, tensile properties of each single-aligned discontinuous fibre composite were measured except for the high modulus carbon fibre composites (Granoc XN-90, NGF, Japan), as the piping system of the prototype rig for the HiPerDiF method was not suitable when only this type of fibre

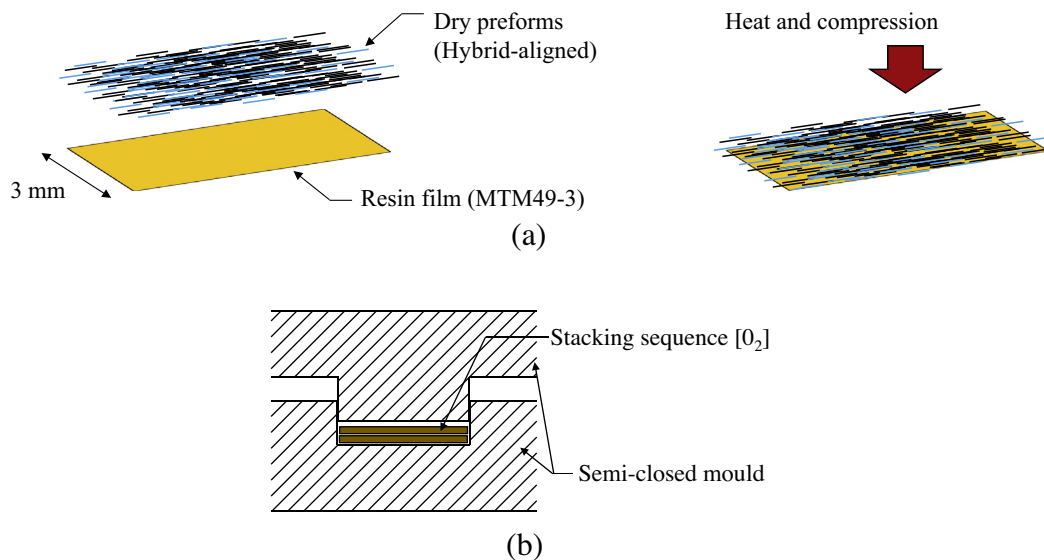


**Fig. 5.** Pre-processing (a) and stacking sequence (b) for fabricating hybrid composite specimens. (For interpretation of the references to colour in this figure legend, the reader is referred to the web version of this article.)

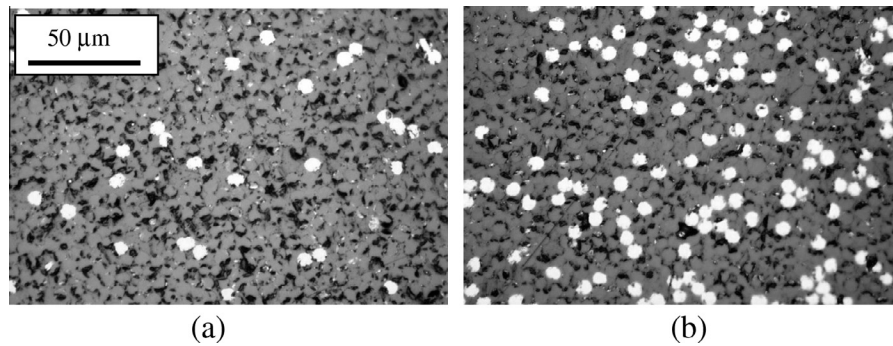


**Fig. 6.** Cross section images of high strength carbon/E-glass composite samples, relative carbon ratio: (a) 0.1, (b) 0.2. Carbon fibres appear white.

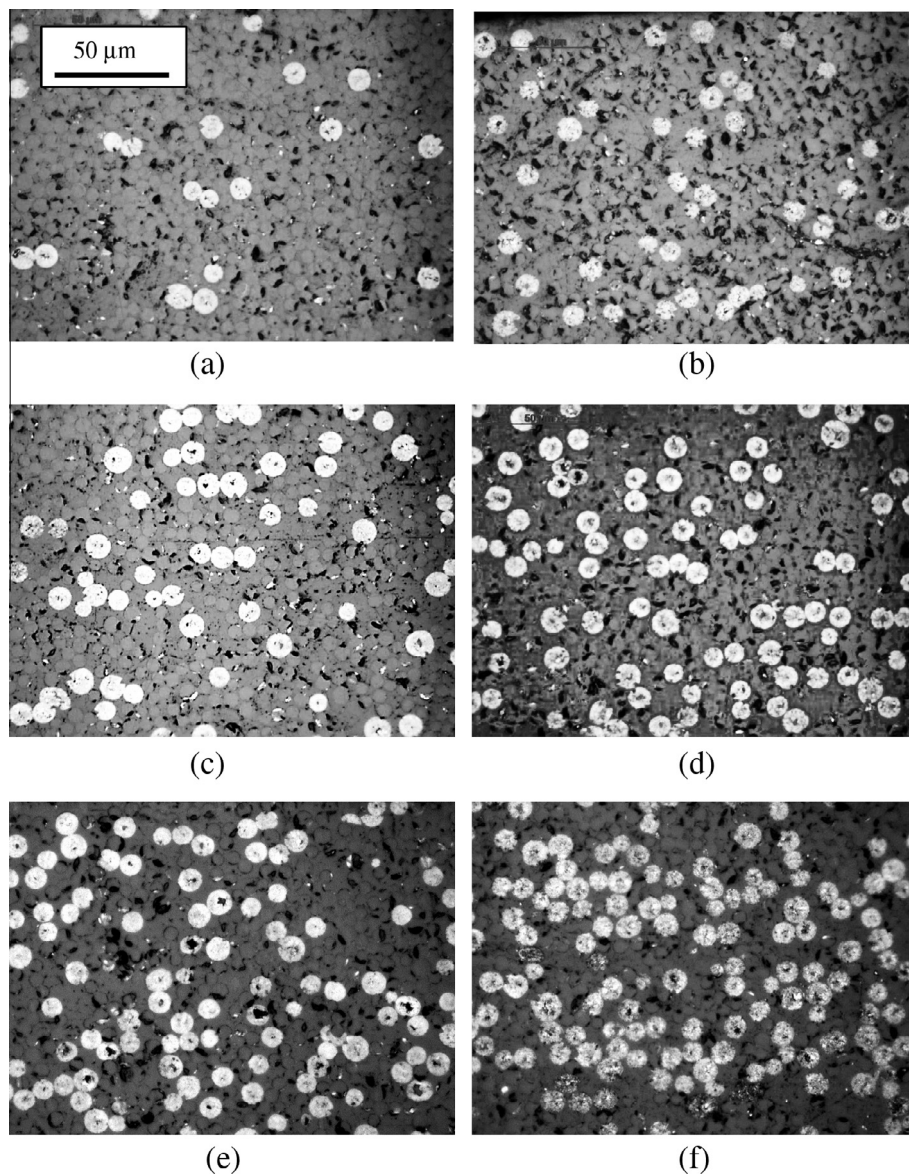


**Fig. 7.** Cross section images of high modulus carbon/E-glass composite samples, relative carbon ratio: (a) 0.1, (b) 0.2, (c) 0.25, (d) 0.33, (e) 0.4, (f) 0.5. Carbon fibres appear white.

was suspended in water. High strength (HS) carbon/E-glass and high modulus (HM) carbon/E-glass hybrid specimens were prepared with a range of relative carbon volume ratios to study its effect on the pseudo-ductile response. The manufacturing

conditions for the aligned hybrid preforms in the HiPerDiF method are listed in [Table 2](#).

The aligned hybrid preforms were placed onto an epoxy resin film (MTM49-3, Cytec) and then heat and pressure were applied

so that the resin could penetrate into the preform as shown in Fig. 5(a). The specimens were laminated with the stacking sequence shown in Fig. 5(b) and placed in a semi-closed mould. The specimens were cured at 135 °C for 90 min in an autoclave using vacuum bag moulding under 2.15 MPa pressure. Figs. 6 and 7 show the cross section images of the cured hybrid composite specimens. The carbon fibres and glass fibres appear white and grey respectively. After curing and before the tabbing process for the tensile test, burrs at all edges along the fibre direction were gently removed using sand paper. Glass fibre/epoxy end tabs were attached to the specimens using epoxy adhesive, Redux®, Hexcel. The specimen dimensions are illustrated in Fig. 8 and the thicknesses of specimens are listed in Table 2.

### 3.2. Tensile test

Tensile tests were performed on an electro-mechanical testing machine with a cross-head displacement speed of 1 mm/min. The load was measured with a 10 kN load cell (Shimadzu, Japan) and the strain was measured with a video extensometer (IMETRUM, UK). White dots were painted on the specimens to allow the strain measurement with the video extensometer. The gauge length for the strain measurement was 15 mm.

## 4. Results and discussion

### 4.1. High strength carbon/E-glass hybrids

In the present work, the stress–strain curves for the high strength carbon/E-glass hybrids were predicted according to Jalalvand's model, ignoring any potential hybrid effect, as shown in Fig. 9(a). If the failure strain of the low elongation constituent is assumed the same as the failure strain of the aligned discontinuous carbon composite ( $\epsilon_{sc}$ , 1.41%), the hybrid with 0.1 relative carbon ratio can produce a fragmentation plateau in the hybrid composites stress–strain curve while 0.2 relative carbon ratio shows a catastrophic. However, no stiffness reduction or deviation from the initial elastic line was observed which means that the failure strain of the high strength carbon/E-glass hybrid composites reached the failure strain of the carbon fibre ( $\epsilon_{cf\_HS}$ , 1.9%) with no substantial carbon fibre fragmentation. Fig. 9(b) shows representative stress–strain curves obtained from the tests as well as the expected response assuming a value of carbon fibre failure strain equal to 1.9%. The analytical predictions, assuming that  $\epsilon_{Lu} = \epsilon_{cf\_HS}$ , show a reasonable agreement with the experimental tensile response although the experimentally measured modulus of the specimens with 0.2 relative carbon ratio is larger than the

predicted value based on the rule of mixtures. In reality, the actual carbon ratio was probably slightly higher than 0.2. The average failure strain of the hybrid composite is higher than the measured failure strain of the single short carbon fibre composites (1.41%). The obtained failure is catastrophic mainly because the failure strain of the high strength carbon fibres is 1.9% which is very close to the failure strain of the E-glass short fibre composites in tension; therefore, when these two fibres are mixed, the obtained hybrid composites do not show a plateau region in the stress–strain curves. All longitudinal properties of the high strength carbon/E-glass hybrid composites in tension are listed in Table 3.

### 4.2. High modulus carbon/E-glass hybrids

The hardening effect of the aligned high modulus carbon short fibre composites in the hybrids is estimated to be 280 GPa using a linear fit to the initial modulus of the hybrid composites as a function of the relative carbon volume ratio, as shown in Fig. 10(a). This is because the modulus of intermingled hybrid composites follows a combination of “parallel” and “series” rule of mixtures, particularly when the two types of fibre have a big difference

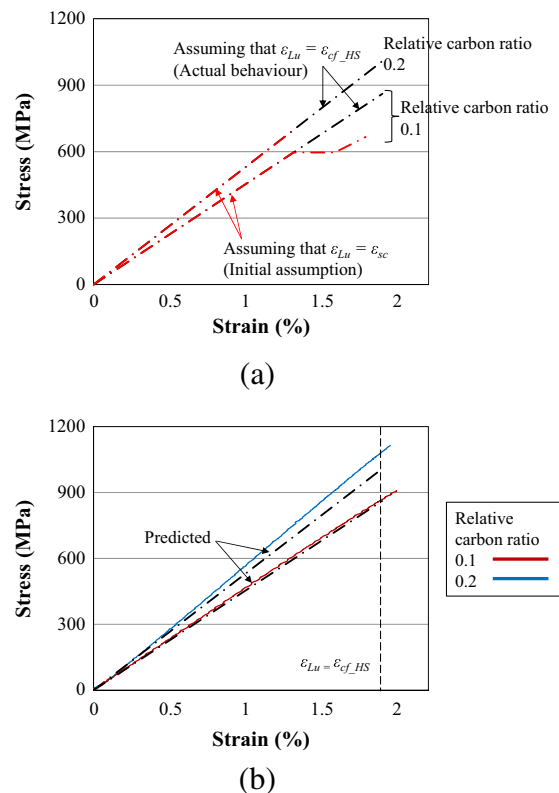


**Fig. 9.** (a) Predicted stress–strain curves and (b) representative stress–strain curves of high strength carbon/E-glass composite samples with 0.1 and 0.2 relative carbon ratio. (For interpretation of the references to colour in this figure legend, the reader is referred to the web version of this article.)

**Table 3**

Tensile properties of high strength carbon/E-glass hybrid composites.

Relative carbon ratio	0.1			0.2		
	<i>E</i> (GPa)	$\sigma_U$ (MPa)	$\epsilon$ (%)	<i>E</i> (GPa)	$\sigma_U$ (MPa)	$\epsilon$ (%)
Mean	46.0	917	2.01	61.7	1080	1.77
SD	1.23	24.0	0.03	2.62	76.9	0.17
CV (%)	2.7	2.6	1.4	4.3	7.1	8.9

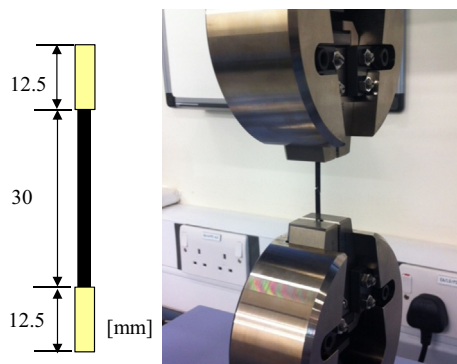


**Fig. 8.** Hybrid composites specimen schematic and tensile test set-up (Width = 3 mm). (For interpretation of the references to colour in this figure legend, the reader is referred to the web version of this article.)

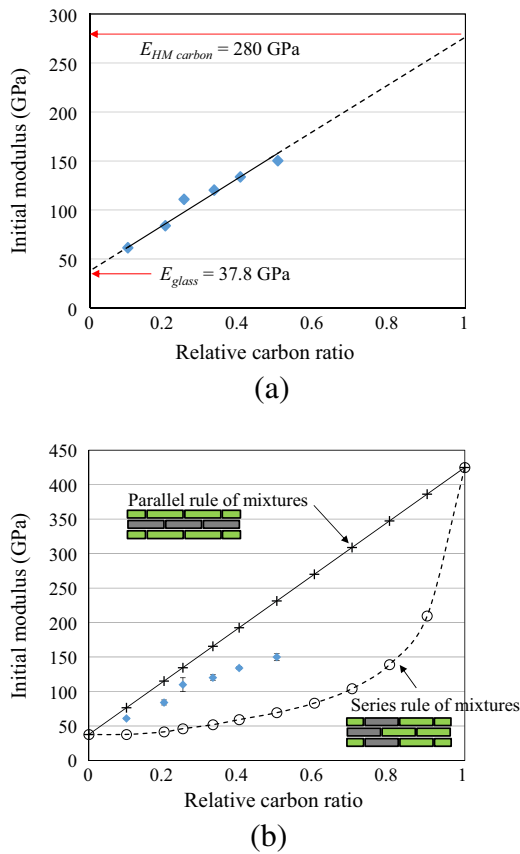


**Fig. 10.** (a) Stiffening effect of the high modulus carbon composite in intermingled hybrids, (b) initial modulus of high modulus carbon/E-glass hybrid composites ( $\pm 1$  SD) as a function of the relative carbon ratio with theoretical initial modulus graphs based on the parallel and series rule of mixtures. (For interpretation of the references to colour in this figure legend, the reader is referred to the web version of this article.)

in their modulus. The blue diamond markers in Fig. 10(b) represent the experimental results of the intermingled hybrid composites, which are in between two extreme cases: parallel rule of mixtures shown with “+” and series rule of mixtures depicted by “o”. Fig. 11(a) shows the predicted tensile stress–strain curves for different relative carbon volume ratios when the failure strain of the low elongation constituent is assumed equal to the failure strain of the high modulus carbon fibre and Fig. 11(b) shows the experimental tensile stress–strain curves. The pseudo-ductile properties of each case, summarised in Table 4, were measured based on the definition suggested by Wisnom et al. [17,31]. The yield point ( $\sigma_Y$ ) was defined as the intersection of the stress–strain curve and a straight line with the same initial slope and 0.1% offset from the origin, as shown in Fig. 12. This definition is equivalent to the definition of proof stress in metals.  $\epsilon_{max}$  is the strain at which the specimen loses its integrity. The pseudo-ductile strain,  $\epsilon_d$ , is the difference between  $\epsilon_{max}$  and the elastic strain,  $\epsilon_{E0}$ , at the same stress level based on the initial modulus,  $E_0$ , as illustrated in Fig. 12. The failure strain of the low elongation constituent is identified from the slope change of the stress–strain curves, as shown in Fig. 13. Comparing the stress–strain curves of hybrids with low and high carbon volume ratio, a different shape of the transition between the elastic deformation and the fragmentation plateau can be observed. In the specimens with low relative carbon volume ratios, where most of the carbon fibres are surrounded by glass fibres as shown in Fig. 7(a) and (b) there is little carbon clustering. Therefore each carbon fibre fragments individually, the results in a very smooth transition between the elastic and fragmentation

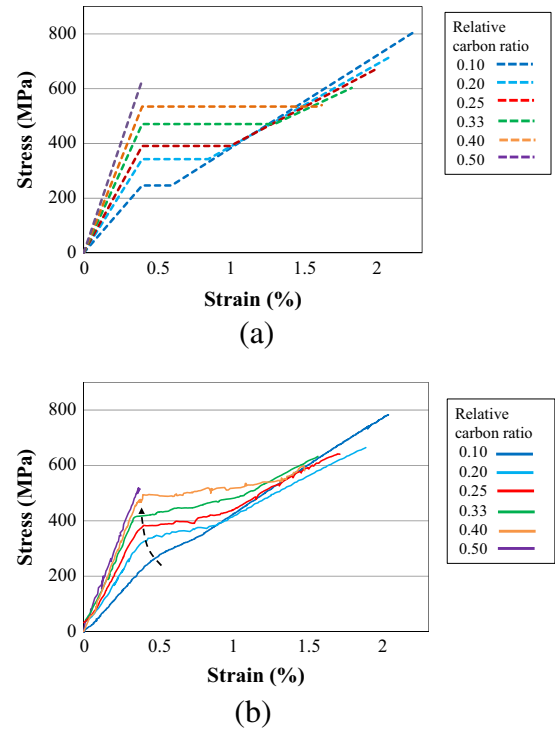


**Fig. 11.** (a) Predicted stress–strain curves according to Jalalvand model and (b) representative stress–strain curves of high modulus carbon/E-glass composite samples with different relative carbon ratio. (For interpretation of the references to colour in this figure legend, the reader is referred to the web version of this article.)

**Table 4**

Pseudo-ductile properties of high modulus carbon/E-glass hybrid composites.

Relative carbon ratio	$E_0$ (GPa) (CV%)	$\sigma_Y$ (MPa) (CV%)	$\epsilon_Y$ (%)	$\sigma_U$ (MPa) (CV%)	$\epsilon_{max}$ (%) (CV%)	$\epsilon_d$ (%) ( $=\epsilon_{max} - \epsilon_{E0}$ )
0.1	61.0 (2.42)	312 (3.99)	0.616	743 (8.85)	2.00 (6.72)	0.679
0.2	84.0 (4.38)	346 (3.35)	0.511	635 (3.73)	1.80 (8.05)	1.01
0.25	110 (8.9)	400 (2.69)	0.464	690 (4.82)	1.72 (6.11)	1.10
0.33	120 (3.45)	419 (4.81)	0.458	614 (4.73)	1.53 (5.68)	1.00
0.4	134 (1.64)	441 (5.92)	0.434	542 (7.47)	1.29 (15.2)	0.879
0.5	150 (3.50)	–	–	466 (10.0)	0.323 (8.68)	–

plateaus in the stress–strain curve. The apparent failure strain of the low elongation constituent is slightly higher than the nominal failure strain of the high modulus carbon fibres ( $\epsilon_{cf-HM}$ ), as shown in Fig. 13, because catastrophic crack propagation is prevented by the intervening glass fibres (high elongation constituent) after the failure of a few carbon fibres. When the carbon volume ratio is increased there is a sharp transition between the elastic region and the fragmentation plateau and the low elongation constituent failure occurs at strains lower than the nominal failure strain of the high modulus carbon fibres, as shown in Fig. 13. This is because clusters of carbon fibres that break simultaneously appear in the hybrid cross section, as shown in Fig. 7(c)–(e). Bigger carbon clusters result in longer crack spacing; a lower number of cracks is required to reach a crack saturated state in the composite. Therefore, each crack in a bigger cluster of carbon fibres can cause

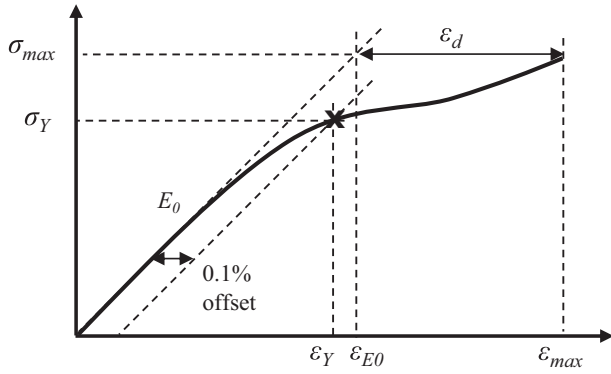


Fig. 12. Definition of pseudo-ductile properties for composites.

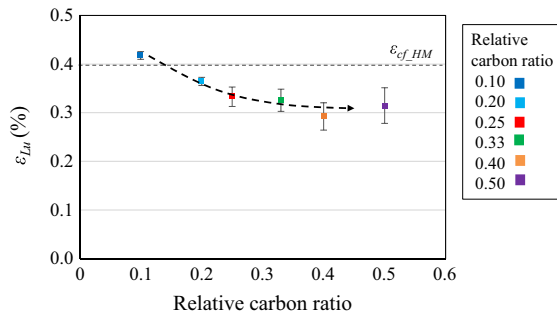


Fig. 13. The apparent failure strain of the low elongation constituent experimentally measured for hybrids with  $\pm 1$  SD as a function of the relative carbon ratio. (For interpretation of the references to colour in this figure legend, the reader is referred to the web version of this article.)

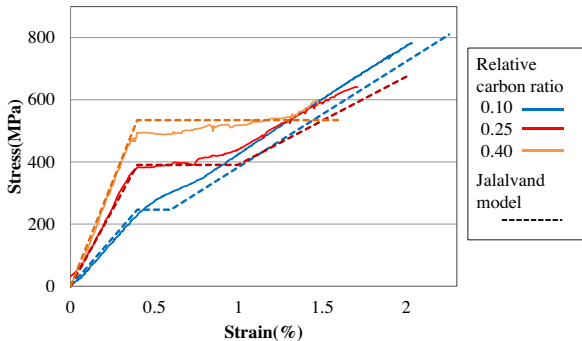


Fig. 14. Representative stress–strain curves of high modulus carbon/E-glass hybrid composites with 0.1, 0.25 and 0.4 relative carbon ratio with predicted curves. (For interpretation of the references to colour in this figure legend, the reader is referred to the web version of this article.)

a more significant slope change in the stress–strain curve. When the hybrid composite has equal amounts of carbon and glass fibres (i.e. relative carbon ratio of 0.5), the overall behaviour is elastic-brittle because the glass fibres cannot carry the applied load after the carbon fibres fail and the stress–strain curve does not show a fragmentation plateau.

The experimental and the analytical model results in Fig. 10 shows a good agreement. Fig. 14 compares representative experimental stress–strain curves and the predicted stress–strain curves from the analytical solution. The difference in the shape of the transition point between the elastic region and the fragmentation plateau can be explained considering that the model does not take

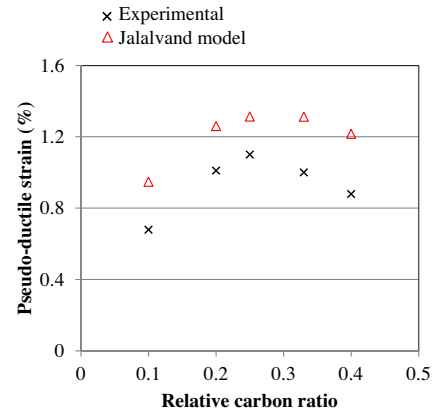


Fig. 15. Pseudo-ductile strain of hybrids with the predicted values from the analytical model. (For interpretation of the references to colour in this figure legend, the reader is referred to the web version of this article.)

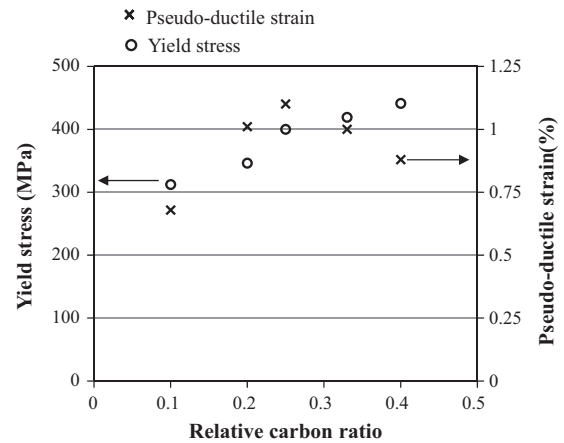


Fig. 16. Yield stress and pseudo-ductile strain of intermingled hybrids as function of the relative carbon ratio.

into account the clusters and uses a single failure stress,  $\sigma_{@LFrags}$  and not a statistical distribution. The observed pseudo-ductile strains are slightly less than the predicted values. It has to be remarked that Jalalvand's model was developed initially for continuous hybrid composites. Since the short fibre length is significantly higher than the critical length, the model can be applied to the current case to estimate the intermingled short fibre composite global response, i.e. initial modulus and fragmentation stress. However when predicting the pseudo-ductile strain it must be borne in mind that discontinuities are present in the structure of the aligned short fibres specimens along the loading direction, therefore not all the fragmentations predicted by the analytical model can take place. However, the analytical prediction is a good estimation of the overall behaviour of the hybrid. It also well predicts the relative carbon volume ratio that gives the maximum pseudo-ductile strain for the discontinuous fibre composites. In this particular hybrid composite with high modulus carbon and E-glass fibres, when the relative carbon ratio is 0.25, the pseudo-ductile strain reaches a maximum value of 1.1%, the yield strength is 400 MPa and the tensile modulus 110 GPa, as shown in Figs. 15 and 16. Moreover, the initial modulus of aligned short fibres hybrid composites with 0.4 relative carbon volume ratio is 134 GPa, 3.5 times higher than that of E-glass–epoxy composites. The stress–strain curve shows pseudo-ductile behaviour with a clear “yield point” at 441 MPa and a well dispersed and gradual damage process.

## 5. Conclusion

Aligned short fibre hybrid composites with high strength carbon/E-glass fibres and high modulus carbon/E-glass fibres were successfully produced using the HiPerDiF method [26]. When loaded in tension, high strength carbon/E-glass composites did not show any pseudo-ductility because the failure strain of the carbon fibres was almost the same as the failure strain of the aligned discontinuous glass composite. On the other hand, pseudo-ductility was obtained from the intermingled hybrid composites using high modulus carbon/E-glass fibres. They were manufactured with relative carbon volume ratios of 0.1, 0.2, 0.25, 0.33, 0.4 and 0.5 and tested in tension in order to investigate the carbon ratio effect on the stress–strain curve. The observed pseudo-ductile strains, as a result of the fragmentation in the low elongation constituent (carbon), were in good agreement with the simple analytical solution. The fragmentation strain was related to the volume and moduli ratios and the failure strain of the low elongation constituent. In addition, the results of intermingled high modulus carbon/E-glass composites have clearly confirmed that the apparent failure strain of the low elongation constituent increases in low relative carbon volume ratios. When the relative carbon ratio was 0.25, the pseudo-ductile strain reached the maximum value, 1.1%, with 400 MPa yield stress, 690 MPa strength and 110 GPa tensile modulus. This study of intermingled hybrid composites shows that the HiPerDiF method is a powerful approach to develop and investigate new hybrid materials allowing variation of fibre types, length and dispersion state.

## Acknowledgements

This work was funded under the UK Engineering and Physical Sciences Research Council (EPSRC) Programme Grant EP/I02946X/1 on High Performance Ductile Composite Technology in collaboration with Imperial College, London.

## References

- [1] Bradley PD, Harris SJ. Strategic reinforcement of hybrid carbon fiber-reinforced polymer composites. *J Mater Sci* 1977;12(12):2401–10.
- [2] Bunsell AR, Harris B. Hybrid carbon and glass fibre composites. *Composites* 1974;5:157–64.
- [3] Chou T-W. Microstructural design of fiber composites. Cambridge solid state science series. Cambridge; New York: Cambridge University Press; 2005.
- [4] Kretsis G. A review of the tensile, compressive, flexural and shear properties of hybrid fiber-reinforced plastics. *Composites* 1987;18(1):13–23.
- [5] Aveston J, Kelly A. Tensile 1st cracking strain and strength of hybrid composites and laminates. *Philos T R Soc A* 1980;294(1411):519–34.
- [6] Aveston J, Sillwood JM. Synergistic fiber strengthening in hybrid composites. *J Mater Sci* 1976;11(10):1877–83.
- [7] Manders PW, Bader MG. The strength of hybrid glass–carbon fiber composites. 1. Failure strain enhancement and failure mode. *J Mater Sci* 1981;16(8):2233–45.
- [8] Richter H. Single fibre and hybrid composites with aligned discontinuous fibres in polymer matrix. In: Proceedings of ICCM3-3rd International conference on composite materials. Paris, France; 1979. p. 387–97.
- [9] Fukuda H, Chou TW. Monte-Carlo simulation of the strength of hybrid composites. *J Compos Mater* 1982;16:371–85.
- [10] Marom G, Fischer S, Tuler FR, Wagner HD. Hybrid effects in composites – conditions for positive or negative effects versus rule-of-mixtures behavior. *J Mater Sci* 1978;13(7):1419–26.
- [11] Parratt NJ, Potter KD. Mechanical behaviour of intimately-mixed hybrid composites. In: Proceedings of ICCM3-3rd International conference on composite materials. Paris, France; 1979. p. 313–23.
- [12] Summerscales J, Short D. Carbon-fiber and glass-fiber hybrid reinforced-plastics. *Composites* 1978;9(3):157–66.
- [13] Manders PW, Bader MG. The strength of hybrid glass–carbon fiber composites. 2. A statistical-model. *J Mater Sci* 1981;16(8):2246–56.
- [14] Zweben C. Tensile-strength of hybrid composites. *J Mater Sci* 1977;12(7):1325–37.
- [15] Czél G, Wisnom MR. Demonstration of pseudo-ductility in high performance glass/epoxy composites by hybridisation with thin-ply carbon prepreg. *Compos Part A: Appl Sci Manuf* 2013;52:23–30.
- [16] Jalalvand M, Czél G, Wisnom MR. Numerical modelling of the damage modes in UD thin carbon/glass hybrid laminates. *Compos Sci Technol* 2014;94:39–47.
- [17] Jalalvand M, Czél G, Wisnom MR. Damage analysis of pseudo-ductile thin-ply UD hybrid composites—a new analytical method. *Compos Part A: Appl Sci Manuf* 2015;69:83–93.
- [18] Wisnom MR, Czél G, Jalalvand M. Creating more gradual failure in high performance composites via hybridisation. In: Proceedings of the American society for composites; 2013.
- [19] Molazemhosseini A, Tourani H, Khavandi A, Yekta BE. Tribological performance of PEEK based hybrid composites reinforced with short carbon fibers and nano-silica. *Wear* 2013;303(1–2):397–404.
- [20] Diez-Pascual AM, Naffakh M, Marco C, Gomez-Fatou MA, Ellis GJ. Multiscale fiber-reinforced thermoplastic composites incorporating carbon nanotubes: a review. *Curr Opin Solid State Mater Sci* 2014;18(2):62–80.
- [21] Harris B, Bunsell AR. Impact properties of glass fibre/carbon fibre hybrid composites. *Composites* 1975;6:197–201.
- [22] Diao H, Bismarck A, Robinson P, Wisnom MR. Production of continuous intermingled CF/GF hybrid composite via fibre tow spreading technology. In: Proceedings of ECCM16-16th European conference on composite materials. Seville, Spain; 2014.
- [23] Swolfs Y, Crauwels L, Van Breda E, Gorbatikh L, Hine P, Ward I, et al. Tensile behaviour of intralayer hybrid composites of carbon fibre and self-reinforced polypropylene. *Compos Part A: Appl Sci Manuf* 2014;59:78–84.
- [24] Mader E, Rausch J, Schmidt N. Commingled yarns – processing aspects and tailored surfaces of polypropylene/glass composites. *Compos Part A: Appl Sci Manuf* 2008;39(4):612–23.
- [25] Sonparote PW, Lakkad SC. Mechanical-properties of carbon glass-fiber reinforced hybrids. *Fibre Sci Technol* 1982;16(4):309–12.
- [26] Yu H, Potter KD, Wisnom MR. A novel manufacturing method for aligned discontinuous fibre composites (high performance-discontinuous fibre method). *Compos Part A: Appl Sci Manuf* 2014;65:175–85.
- [27] Yu H, Potter KD. Discontinuous fibre alignment method, high performance-discontinuous fibre (HiPerDiF) method. UK application number 1306762.4; 2013.
- [28] Yu H, Potter KD, Wisnom MR. A novel manufacturing method of aligned short fibre composite. In: Proceedings of ECCM15-15th European conference on composite materials. Venice, Italy; 2012.
- [29] Yu H, Potter KD, Wisnom MR. Aligned short fibre composites with high performance. In: Proceedings of ICCM19-19th International conference on composite materials. Montreal, Canada; 2013.
- [30] Yu H, Jalalvand M, Wisnom MR, Potter KD. Hybrid composites with aligned discontinuous fibres. In: Proceedings of ECCM16-16th European conference on composite materials. Seville, Spain; 2014.
- [31] Czél G, Jalalvand M, Wisnom MR. Development of pseudo-ductile hybrid composites with discontinuous carbon and continuous glass prepreps. In: Proceedings of ECCM16-16th European conference on composite materials. Seville, Spain; 2014.